LWT - Food Science and Technology 194 (2024) 115809

Contents lists available at ScienceDirect

LWT

journal homepage: www.elsevier.com/locate/lwt

Optimization of an onion oil microemulsion by response surface methodology for enhanced physicochemical stability and biological activity

Enrique Guillamon Ayala [a], Borja Domínguez Martín [a], Nuria Mut-Salud [b], Javier M. Ochando-Pulido [c], José Antonio Morales-González [c], Alberto Baños Arjona [b], Antonio Martinez-Ferez [c,*]

[a] Department of Chemistry, DMC Research Center SLU, 18620, Granada, Spain
[b] Department of Biotechnology, DMC Research Center SLU, 18620, Granada, Spain
[c] Chemical Engineering Department, University of Granada, Avenida Fuentenueva S/n, 18071, Granada, Spain

ARTICLE INFO

Keywords:
Onion oil
Microemulsion
Stability
Antitumor
Anti-inflammatory

ABSTRACT

Onion oil (OO) containing propyl-propane thiosulfinate (PTS) and propyl-propane thiosulfonate (PTSO) is known for various therapeutic properties. However, its industrial use in hydrophilic matrices is challenging due to the lack of physicochemical stability. Applying Box-Behnken design (BBD), we developed an optimal OO microemulsion (OOME) with a minimum droplet size and maximum chemical stability. The OOME comprised 2 % w/w oily phase (high oleic acid sunflower oil), 120 mg/L of OO containing PTS+PTSO, 1.47 % w/w emulsifier (Diacetyl tartaric acid ester of mono-diglycerides, DATEM), 0.25 % stabilizer (xanthan gum) and 573 mM phosphate buffer. Turbidimetry as well as laser and dynamic light scattering over 30 days was used to characterize physical stability of the OOME, assessing chemical stability by HPLC. Cytotoxicity and quantification of cytokines (IL-4 and IL-8) were evaluated in colorectal cancer cells (HT-29, T-84 and SW-837) culture supernatants. After 30 days of storage, OOME remained stable, with no flocculation or coalescence phenomena. It achieved a PTS+PTSO amount of 98 mg/L, a droplet size of 329 nm, a particle size dispersal coefficient of 0.89, and Z-potential was −40.17 mV. The OOME improved the antitumor effect of OO in lines HT-29 and SW-837, as well as its influence on the inflammatory response.

1. Introduction

The term "nutraceutical" defines those dietary compounds which have physiological benefits or provide some protection against chronic diseases (Gupta & Prakash, 2015). Among nutraceuticals, plant-derived compounds, or phytochemicals, play a key role. Epidemiological evidence has shown that these substances exert protective effects against infections, tumours, and cardiovascular diseases (Girish Sharma et al., 2014). Therefore, the supplementation with phytochemicals in food systems is a simple method to develop innovative functional foods or supplements that may improve health status. Some of the phytochemicals traditionally used are organosulfur compounds (OSCs), like glucosinolates from Brassica vegetables, or (poly)sulfides, thiosulfinates and thiosulfonates present in *Allium* species such as garlic or onion. Onion (*Allium cepa*) is widely consumed and, behind tomatoes, it is the second most developed agricultural crop worldwide. It also has a long history of use as a medicinal plant, as reported on writings since ancient Egypt, and its health benefits have been widely demonstrated in contemporary studies (Kianian et al., 2021). These benefits stem from their diversity in bioactive compounds, such as fibers, quercetin, vitamin C or OSCs (Arshad et al., 2017). One of the most common OSCs in onions is propiin (S-propyl-L-cysteine sulfoxide), that forms PTS when is in contact with the enzyme alliinase. Despite being more stable than other thiosulfinates such as allicin form garlic, PTS is a labile compound that changes into dipropyl disulfide and PTSO through disproportionation reactions (Guillamon, 2018) (Fig. 1). Some biological properties of PTS and PTSO have been recently reported, including their antimicrobial and hypocholesterolemic effects (Sorlozano-Puerto et al., 2020; Vezza et al., 2021), or their antitumor and immunomodulatory activity (Guillamón et al., 2023).

However, the incorporation of OO in foods or supplements is a challenging issue due to its low water solubility and high susceptibility

* Corresponding author.
E-mail addresses: Enrique.guillamon@dmcrc.com (E. Guillamon Ayala), amferez@ugr.es (A. Martinez-Ferez).

https://doi.org/10.1016/j.lwt.2024.115809
Received 30 October 2023; Received in revised form 28 December 2023; Accepted 27 January 2024
Available online 29 January 2024

to chemical degradation or hydrolisis (Nagy & Winterbourn, 2010). Thus, in order to overcome these limitations, proper formulations must be developed to ensure that these OSCs may exert their beneficial effects. Among delivery systems for this purpose, the food industry still prefers microemulsions, especially in the case of drinkable single-dose supplements like sachets (Arredondo-Ochoa & Silva-Martínez, 2022). Emulsions are stable suspensions of two immiscible liquids, obtained by the dispersion of very fine drops of a liquid (dispersed phase) in another (continuous phase). The two predominant types of emulsions are oil-in-water (O/W) and water-in-oil (W/O). Emulsions are thermodynamically unstable and phases tend to separate through time by different phenomena including coalescence or flocculation (Kumar et al., 2022). The stability of emulsions is highly affected by the aggregation of droplets, and can be improved by reducing the droplet size, as occurs in microemulsions (MEs). MEs, with droplet diameters from 100 to 400 nm, show other advantages, as higher of interface area and ease of production using different techniques, such as homogenizers (high--pressure or rotor-stator) or ultrasonication (Souto et al., 2022). The stability of MEs can also be enhanced by adding emulsifiers, that decrease surface tension and avoid droplet flocculation, or stabilizers, like hydrocolloids, that increase the viscosity of the aqueous phase and enlarge the spatial repulsive force between oil droplets (McClements & Jafari, 2018). Due to this high number of elements involved in the stability of emulsions, the application of response surface methodologies (RSMs), as BBD, is highly recommended for predicting and optimizing the composition, properties and processing conditions of MEs.

Therefore, the aims of this study were to: i) optimize the formulation applying a Box-Behnken design to obtain a stable OOME by rotor-stator homogenization to ensure a minimum droplet size and maximum chemical stability; ii) characterize the optimal OOME in terms of physicochemical properties and stability; iii) evaluate the *in vitro* antiproliferative activity of the OOME in colorectal carcinoma cell lines; and iiii) evaluate the effect of different concentrations of the OOME on the level of cytokines IL-8 and IL-4 produced by HT-29 cells.

2. Materials and methods

2.1. Materials

Pure PTS and PTSO (purity>98 %), OO (content in PTS+PTSO >92 %) and High oleic acid sunflower oil (SO) were supplied by DOMCA S.A. U. (Granada, Spain). Sodium hydroxide, xanthan gum (XG) and phosphate buffer were purchased from Sigma-Aldrich (St. Louis, USA). Diacetyl tartaric acid ester of mono-diglycerides (DATEM, trademark Panodan® SD/D K), was supplied by Du Pont Danisco (Copenhagen, Denmark).

2.2. Microemulsion preparation

Diluted O/W emulsions (2 % w/w of dispersed phase; all percentages referred in this work are expressed in w/w) were prepared with a rotor-stator homogenizer (UNIDRIVE X 1000, F T20, Ingenieurbüro CAT, M. Zipperer GmbH, Germany). Firstly, 24 h prior to the OOME preparation, XG was hydrated in the buffered-water, adjusted to pH 7 with sodium hydroxide. Secondly, in another beaker, OO was mixed with SO at an amount of 6 g/kg. The selected emulsifier was then slowly added into the continuous phase, avoiding foam formation. Finally, as represented

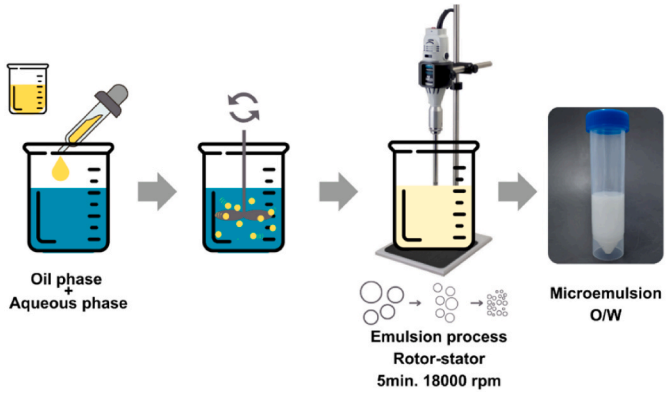

Fig. 2. Outline of the emulsification process.

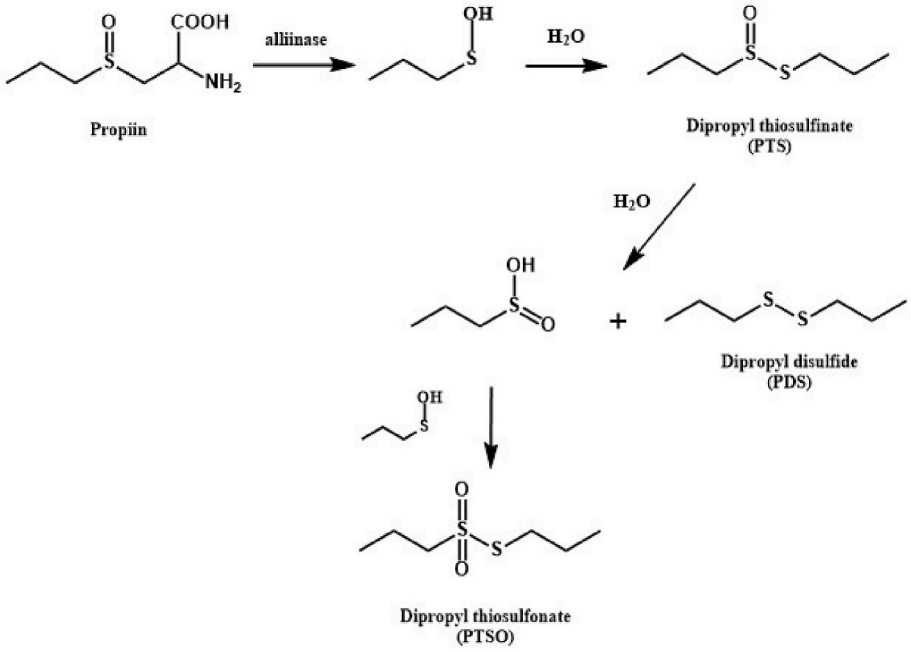

Fig. 1. Organosulfur compounds derived from propiin in onion.

in Fig. 2, the dispersed phase including the OO was slowly added using a Pasteur pipette. Homogenization process was kept at 18000 rpm for 5 min.

2.3. Experimental design and microemulsion optimization by BBD

BBD was employed to examine the effect of the main independent variables on response variables. The key process parameters considered and selected, including the emulsifier chosen, the emulsifier-OO ratio, organic phase-aqueous phase ratio, emulsification time, agitation speed, pH and buffer concentration, were all investigated by single factor experiments. On the basis of their results, three major input factors were confirmed – emulsifier concentration (A), XG concentration (B) and phosphate buffer dosage (C) – in terms of their effects on the response variables to be optimized: the droplet size and the concentration of active ingredients (AIC), expressed as the sum of PTS+PTSO in mg/L. Our BBD comprised a total number of 15 experiments, with three central points and three replicates. The input factors considered for this study, arranged into three levels, are reported in Table 1.

2.4. Methods for characterization of microemulsion

2.4.1. Size distribution of oil droplets

The OOME particle size was determined by measuring the mean droplet size after their preparation and storage at 25 ± 1 °C for 30 days. The measures were weekly performed with a laser light scattering (LLS) Mastersizer 3000 diffractometer (Malvern Instruments, Worcestershire, UK). The droplet size was characterized by distribution curves in volume (%) *vs.* droplet diameter, utilizing De Broukere mean ($d_{4,3}$ index), defined as $\Sigma n_i d_i^{\ 4}/\Sigma n_i d_i^3$. The particle size dispersal coefficient (span) was also reported, defined as $(d_{90}\text{-}d_{10})/d_{50}$, where d_{90}, d_{10} and d_{50} are the respective diameters at 10, 50, and 90 % of the cumulative droplet distribution or oil volume (Santos et al., 2022).

Emulsions were prepared 24 h before the test. The optical parameters selected were a continuous-phase refractive index of 1.333 (water refractive index) and a dispersed-phase refractive index of 1.469 (SO refractive index). The emulsions were introduced in the diffractometer cell at 25 ± 1 °C, under moderate stirring to reach 10–20 % laser obscuration value. Droplet size measurements were carried out in quadruplicate and results were disclosed as average $d_{4,3}$.

Table 1
Experimental values of particle size and AIC (expressed as concentration of PTS+PTSO) of the OOME prepared according to BBD experimental design (levels adopted in the RSM design are presented in brackets).

Sample	$d_{4/3}$ (μm)	AIC (mg/L)	Z-Potential (mV)	Emulsifier (%)	Stabilizer (%)	Buffer (mM)
1	1.03 ± 0.03	84.1 ± 0.4	−16.14	1.5 (0)	0.25 (−1)	700 (1)
2	0.495 ± 0.006	77.5 ± 0.5	−30.07	1.75 (1)	0.375 (0)	100 (-1)
3	3.49 ± 0.21	67.7 ± 0.5	−25.42	1.25 (−1)	0.375 (0)	700 (1)
4	3.51 ± 0.54	71.7 ± 0.7	−18.11	1.75 (1)	0.5 (1)	400 (0)
5	0.904 ± 0.018	73.2 ± 0.7	−27.91	1.25 (−1)	0.25 (−1)	400 (0)
6	3.41 ± 0.15	77.0 ± 1.3	−11.47	1.5 (0)	0.5 (1)	700 (1)
7	14.9 ± 0.7	49.3 ± 0.6	−52.34	1.25 (−1)	0.375 (0)	100 (−1)
8	2.52 ± 0.034	79.2 ± 1.1	−50.12	1.5 (0)	0.25 (−1)	100 (−1)
9	0.867 ± 0.011	85.9 ± 1.0	−24.87	1.5 (0)	0.5 (1)	100 (−1)
10	0.939 ± 0.008	83.7 ± 1.3	−33.09	1.5 (0)	0.375 (0)	400 (0)
11	2.76 ± 0.13	72.9 ± 1.3	−13.39	1.75 (1)	0.5 (1)	400 (0)
12	4.03 ± 0.27	76.2 ± 1.4	−38.61	1.5 (0)	0.375 (0)	400 (0)
13	2.61 ± 0.12	59.2 ± 0.5	−22.18	1.25 (−1)	0.5 (1)	400 (0)
14	6.06 ± 0.6	61.5 ± 0.9	−22.84	1.75 (1)	0.375 (0)	700 (1)
15	0.583 ± 0.009	94.7 ± 0.4	−26.41	1.5 (0)	0.375 (0)	400 (0)

2.4.2. Zeta potential measurement

The zeta potential of the emulsions was determined by using a dynamic light scattering droplet size analyzer (Zetasizer Nano ZS90, Malvern Instruments, Worcestershire, UK). The samples were directly filled into the Zetasizer disposable cells, without any dilution. The measurements were performed with an angle of 173 °C at 25.0 ± 1 °C. Each analysis consisted of three replicates and results were reported as average.

2.4.3. Determination of Turbiscan Stability Index

The physical stability of the optimal OOME was also measured by turbidimetry. Measures were carried out with Turbiscan AGS (Formulaction, L'Union, France), which simultaneously records light transmission and backscattering (BS) on the dispersed oil droplets (Lu et al., 2017). Turbiscan™ detects destabilization phenomena much earlier than the naked eye's operator, enabling faster and more accurate characterization of suspensions compared to visual observation (Carbone et al., 2015). The analyzer is equipped with a pulsed near infrared light source (880 nm) and synchronous optical detectors which determine the intensity of back-scattered light (BS). The emulsion samples (20 mL) were put into a flat-bottomed cylindrical glass vial of 5 cm height and 16 mm diameter, and placed into the measurement chamber. Scans were carried out at 25 °C and at 0, 1, 6, 14, 22 and 30 days since production of OOME. The measurements were repeated three times independently. Turbiscan Stability Index (TSI) was calculated according to Zheng et al. (2018) as $TSI = \sqrt{\frac{\sum_{i=1}^{n}(x_i - x_{BS})^2}{n-1}}$, where x_i is the average BS for each minute of measurement, x_{BS} is the mean value of x_i, and n is the number of scans.

2.4.4. Quantification of bioactive compounds in the emulsion

The determinations of PTSO and PTS were carried out using an Agilent 1260 Infinity HPLC (Agilent Technologies, Inc., CA, USA) and according to a methodology previously developed in our laboratory (Abad et al., 2016). Acetonitrile (HPLC-grade) was supplied by VWR BDH Prolabo (West Chester, PA, U.S.A.). Perchloric acid solution (70 %) was purchased from Sigma-Aldrich (St. Louis, MO, U.S.A.).

2.4.5. Electronic microscopy

Optimal OOME was examined with an Olympus BX51 light polarizing microscope (Olympus, Tokyo, Japan). One drop of the sample was placed between a coverslip and a glass slide and observed under cross-polarized light.

2.5. Biological assays

All chemicals and reagents used in biological assays were purchased from Sigma-Aldrich Química S.L. (Madrid, Spain) unless otherwise stated. All experiments were performed in sextuplicate. In order to analyze whether the constituents of the formulation could interfere with the anti-tumor effect or the production of cytokines, an additional negative control of ME without OO (C-Neg) was also included in the

tests.

2.5.1. Cell lines and culture

HT-29 human colon adenocarcinoma (ATCC HTB-38), T-84 human colon carcinoma (ATCC CCL-248) and SW-837 human rectum adenocarcinoma (ATCC CCL-235) cell lines were obtained from the Cell Cultures Unit of the University of Granada (Granada, Spain). Cells were cultured at 37 °C and humidified atmosphere of 5 % CO_2, in darkness, and with Dulbecco's modified Eagle medium supplemented with 10 % fetal bovine serum (FBS), 10 ml/L penicillin-streptomycin 100x and 2 mM L-glutamine.

2.5.2. In vitro cytotoxicity assays

Cells were seeded in sterile 96-well plates (Thermo Fisher Scientific) at high density ($1.5x10^4$ cells/well) and incubated at 37 °C with 5 % CO_2 for 24h. Increasing concentrations of OO and optimal OOME (to obtain 1–16 mg/L of PTS+PTSO) were added in the wells and incubated for 48h at 37 °C with 5 % CO_2. The effect of the emulsions on tumor colorectal cell lines (HT-29, T-84 and SW-837) was evaluated using a colorimetric technique with sulforhodamine-B (SRB) (Vichai & Kirtikara, 2006).

Optical density values were determined by colorimetry at 490 nm using a microplate reader (Multiskan EX, Thermo Electron Corporation, MA, USA). The assessment of absorbance was performed using "SkanIt" RE 5.0 for Windows v.2.6 (Thermo Labsystems, MA, USA). The half maximal inhibitory concentration (IC_{50}) values were calculated from the semi-logarithmic dose-response curve by linear interpolation.

2.5.3. In vitro anti-inflammatory assays

HT-29 cells were seeded at high density in sterile 96-well plates. After 24 h, supernatants of each well were discarded and different concentrations of OO and optimal OOME were dissolved in the supplemented medium and added in the wells. After 1h of incubation, 10 mg/mL of lipopolysaccharide from *Salmonella enterica* serotype typhimurium (LPS) was added and plates were incubated for 24h at 37 °C and 5 % CO_2. The concentrations evaluated for both products were the ones required to provide 1–16 mg/L of PTS+PTSO. After induction, supernatants were collected, centrifuged at 1000×*g* for 10 min and stored at −80 °C until cytokines (IL-8 and IL-4) determination by ELISA was performed using commercial kits (Invitrogen-ThermoFisher Scientific, MA, USA).

2.6. Statistical analyses

Data were analyzed using STATGRAPHICS Centurion XVI, Statgraphics Technologies Inc., Virginia, USA. An analysis of variance (ANOVA) was performed to identify significant differences between independent variables. The reduced model incorporated statistically significant variables ($P < 0.05$). The optimal conditions for minimizing droplet size ($d_{4/3}$) while maximizing AIC were determined based on the fitted equations. The validity of the proposed model was confirmed by assessing the mean absolute error (MAE) and Durbin-Watson statistic. Additionally, figures and statistical analysis for anti-inflammatory assays were generated with GraphPad prism 8.0 software (La Jolla, CA, USA) using a one-way ANOVA test supplemented with Tukey's post hoc. Differences were considered statistically significant when $p < 0.05$.

3. Results and discussion

3.1. Optimization of OOME using Box-Behnken model

Table 1 shows the factor levels and response data attained for the set of BBD experiments performed, along with the Zeta potential results. After data compilation, F-values, p-values and R^2 for $d_{4/3}$ (Table 2) and AIC (Table 4) were obtained from ANOVA. Curves of the main effects and the response surfaces were obtained for each variable. An optimization of the response variables was performed with the purpose of minimizing $d_{4/3}$ value, while simultaneously maximizing AIC. Along with these results, a multiple response optimization of both outputs was carried out.

Table 2
Analysis of variance for particle size ($d_{4/3}$) of OOME.

Variable	Sum of squares	DF	R^2	*F*-Ratio	*P*-Value
A	19.096	1	19.096	3.11	0.1383
B	9.375	1	9.375	1.53	0.2717
C	2.870	1	2.870	0.47	0.5247
AA	9.180	1	9.180	1.49	0.2761
AB	5.195	1	5.195	0.85	0.4001
AC	72.038	1	72.038	11.72	**0.0188**
BB	20.104	1	20.104	3.27	0.1303
BC	4.066	1	4.066	0.66	0.4530
CC	21.809	1	21.809	3.55	0.1183

A: emulsifier concentration; B: XG concentration; C: phosphate buffer dosage.

Based on ANOVA results obtained for $d_{4/3}$, only the emulsifier interaction with buffer (AC) was significant (p-value = 0.0188), obtaining an R-squared = 83.08 %. The fitted equation obtained was: $d_{4/3} = 119{,}654 - 131{,}489*A + 47{,}6339*B - 0{,}120598*C + 27{,}611*A^2 + 49{,}6971*A*B + 0{,}0565833*A*C - 163{,}444*B^2 + 0{,}0268867*B*C + 0{,}0000295544*C^2$. Moreover, MAE was 1.18. The Durbin-Watson statistic confirmed random variation of the residuals, given that its attained value was 1.7, close to 2, with a p-value equal to 0.3, ensuring no serial autocorrelation among residuals with 95.0 % confidence. Lastly, negligible Lag 1 residuals autocorrelation (0.058), practically zero, pinpointed for no significant structure uncorrelated by the inferred model. The values attained for all these statistical parameters prove the validity of the proposed model as a function of AC. The optimal values found by minimizing $d_{4/3}$ are shown in Table 3.

The effects of emulsifier, stabilizer and buffer on $d_{4/3}$ are shown in Fig. 3. For optimal OOME in terms of $d_{4/3}$, a concentration of emulsifier equal to 1.746 (%), an intermediate value of stabilizer of 0.364 (%) and a low value of buffer of 119.02 (mM) are desirable. Increasing the amount of emulsifier up to a certain point decreases $d_{4/3}$, although it increases again if the emulsifier concentration continues to rise above 1.75 %. This might be explained because, at relatively low concentrations, emulsifier molecules tend to exist as monomers in solution creating a coating around the oil droplets, preventing them from approaching each other and, consequently, reducing physical destabilization mechanisms (Raikos et al., 2017). However, when the emulsifier exceeds a certain value, its molecules spontaneously self-associate and form micelles. This may led to larger droplet size due to an increase in polydispersity in micellar size, which reduces emulsion stability and increases $d_{4/3}$ because of depletion flocculation, as reported earlier (Kori et al., 2021; Yerramilli & Ghosh, 2017).

As long as the stabilizer concentration increases, so does the diameter of the formed drop, reaching a maximum at concentrations around 0.36 %.This is in agreement with Long et al. (2013), who found that low concentrations of XG significantly decreased the droplet size but increasing its concentration might lead to higher $d_{4/3}$ due to self-association of XG and the formation of sub-micelles.

Some authors have pointed out that buffer concentration affects the density and rheology of emulsions and, therefore, may have an impact on droplet diameter. At low values of ionic strength, a transition from sedimentation to suspension (i.e. no gravitational separation) can be

Table 3
Optimization of emulsifier (%), stabilizer (%) and buffer (mM) fixing $d_{4/3}$ to 0.5 μm.

Factor	Lowest	Highest	Optimal
Emulsifier (%)	1.25	1.75	1.746
Stabilizer (%)	0.25	0.5	0.364
Buffer (mM)	100.0	700.0	119.020

Table 4
Analysis of variance for chemical stability (AIC) of OOME.

Variable	Sum of squares	DF	R^2	*F*-Ratio	*P*-Value
A	82.238	1	82.238	1.89	0.2280
B	17.750	1	17.750	0.41	0.5515
C	0.340	1	0.340	0.01	0.9330
AA	892.954	1	892.954	20.48	**0.0063**
AB	27.171	1	27.171	0.62	0.4657
AC	295.840	1	295.840	6.78	**0.0480**
BB	0.826	1	0.826	0.02	0.8959
BC	47.956	1	47.956	1.10	0.3423
CC	45.614	1	45.614	1.05	0.3533

A: emulsifier concentration; B: XG concentration; C: phosphate buffer dosage.

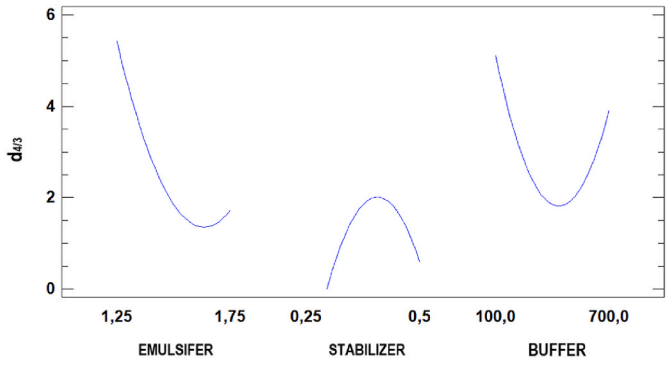

Fig. 3. Effects of emulsifier (%), stabilizer (%) and buffer (mM) on $d_{4/3}$ (μm).

observed due to the modification of rheological properties, but increasing ionic strength brings the electrical charge towards electroneutrality (Dai et al., 2020). This may lead to insufficient long-range electrostatic repulsion forces to prevent the droplets coming in close proximity. As a consequences, the long-range attractive interactions become stronger and may start to cause droplet association. This limiting value was around 573 mM in our work. Indeed, with an excess of ionic strength the structure of XG in solution was also affected, undergoing from a disorder coil to an order helix due, and intermolecular ordering or self-aggregation through hydrogen bonding becomes increasingly significant (Vega et al., 2015).

Maintaining a fixed concentration of buffer at the central point (400 mM), the influence of the emulsifier and the stabilizer on the droplet diameter was assessed using the RSM. As illustrated in Fig. 4, $d_{4/3}$ tended to decrease as the emulsifier concentration was increased, until it becomes asymptotic from 1.7 %. At higher concentrations of emulsifier, the reduction was found to be negligible. In contrast, $d_{4/3}$ increased upon increment of the stabilizer concentration. Ignoring the negative

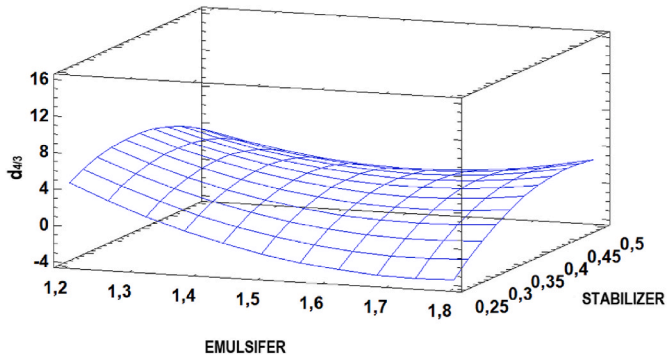

Fig. 4. Estimated response surface for emulsifier (%) and stabilizer (%) concentration optimization on $d_{4/3}$ (μm) of the prepared emulsions for a buffer concentration of 400 mM.

values of the function, with the emulsifier concentration set at around 1.7 %, the optimal stabilizer concentration to attain the minimum $d_{4/3}$ after 30 days was found to be within the range 0.35–0.40 %.

Table 4 shows the ANOVA carried out to assess the chemical stability (AIC) of the OOME. Both the emulsifier concentration (AA) as and the emulsifier/buffer interactions (AC) were significant, with p-values for *AA* of 0.0063 and 0.0480 for *AC*, obtaining an R-square equal to 88.22 %. The fitted equation is: AIC = −566,126 + 835,531*A - 172,638*B + 0,240131*C - 272,319*A^2 + 113,657*A*B - 0,114667*A*C + 33,1238*B^2 - 0,0923333*B*C - 0,0000427414*C^2.

Once again, satisfactory MAE equal to 2.64 was found. The Durbin-Watson statistic confirmed random variation of the residuals, given that its attained value was 1.3, close to 2, with a p-value equal to 0.048, which confirms no serial autocorrelation among residuals with 95.0 % confidence. Moreover, negligible Lag 1 residuals autocorrelation (0.1), practically zero, pinpointed for no significant structure uncorrelated by the inferred model. The values attained for all these statistical parameters prove the validity of the proposed model as a function of AC. Optimal values found for each input factor to maximize the AIC are reported in Table 5.

As it can be noted, to maintain the optimal chemical stability, intermediate values of emulsifier concentration (1.465 %) and of buffer (573.1 mM), together with the lowest concentration of stabilizer (0.25 %) are desirable. Nevertheless, XG concentration had relatively little influence on the stability of PTS+PTSO. Fig. 5 shows the main effects of emulsifier (%), stabilizer (%) and buffer (mM) concentrations on the AIC.

It was detected that the degradation of PTSO+PTS during storage was found to be lower by increasing the concentration of emulsifier up to a certain point (1.47 %), above which AIC decreased. The same was valid for $d_{4/3}$, which increased at high emulsifier concentrations. Therefore, a correlation between physical and chemical stability was observed, in such a way that "destabilization" of the emulsion implies a reduction in chemical stability. This behavior can be explained by the fact that in an emulsion with a low particle size, the OSCs are better protected (Taghavi et al., 2022). However, above a certain concentration of emulsifier, it leads to increased solubilization of OO in water, causing greater degradation by hydrolysis of PTS and PTSO when they get in contact with the external water medium.

In turn, the addition of XG as a stabilizer is essential for obtaining physically stable emulsions over time. XG increases the viscosity of the continuous phase, reduces the Brownian motion between the dispersed droplets and thus maintains stable emulsified components for longer periods (Yang et al., 2017). For this variable, it was noted that the stabilizer decreased the chemical stability, having degraded more PTSO and PTS. In any case, its influence was low. Some authors have pointed out that XG can be adsorbed on the surface of oil droplets, creating a membrane that would inhibit degradation (Cai et al., 2018). However, in our case, XG did not have a protective effect. As XG is not an oxidizing substance nor directly reacts with PTS/PTSO, the reduction in AIC, i.e. chemical stability, is linked to the loss of physical stability.

Regarding the buffer concentration, it was found that an intermediate value in the selected range provides a maximum in chemical stability (Fig. 5). As buffer concentration increases up to a certain point, droplet size decreases, leading to increased chemical stability. By fixing buffer concentration at 400 mM, a value close to the maximum level of AIC, a response surface showing the influence of the emulsifier and the

Table 5
Optimization of emulsifier (%), stabilizer (%) and buffer (mM) upon chemical stability (AIC) equal to 95 mg/L.

Factor	Lowest	Highest	Optimal
Emulsifier (%)	1.25	1.75	1.466
Stabilizer (%)	0.25	0.5	0.250
Buffer (mM)	100.0	700.0	573.114

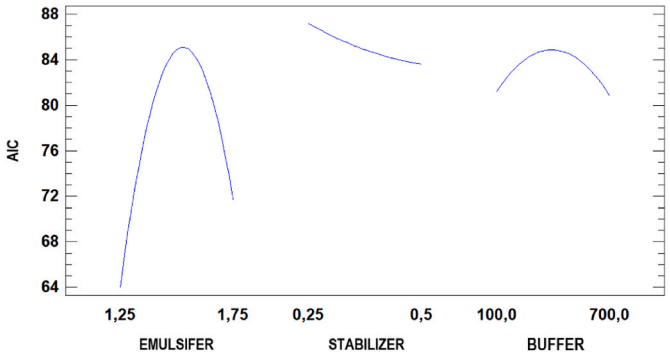

Fig. 5. Effects of emulsifier (%), stabilizer (%) and buffer (mM) on AIC (mg/L).

stabilizer on chemical stability was obtained (Fig. 6).

Lastly, multiple-response optimization was performed. It implied simultaneously minimizing $d_{4/3}$ and maximizing AIC, both variables representing the same weight of 50 %. For this dual optimization, or desirability, the optimal values have been obtained and are presented as follows in Table 6. As it can be noted, results are very similar to the ones obtained to maximize AIC. Therefore, for this OOME to be as stable as possible at a physical and chemical level, an intermediate concentration of emulsifier (1.47 %), a minimum concentration of stabilizer (0.25 %) and a high value of buffer (573 mM) are desirable.

3.2. Characterization of OOME formulation: $d_{4/3}$, span, Z-potential, TSI and microscopy

Using the values provided by multiple-response optimization, an optimal OOME was prepared. The actual values of $d_{4/3}$ and AIC were fairly constant, as shown in Table 7. The data after 30 days since production were found to be 329 ± 1 nm and 98 ± 6 mg/L, which is in close agreement with the predicted values of the model (0.245 μm and 115 mg/L).

The stability of the emulsion is associated with a low value of $d_{4/3}$ but also with a low value of span, since lower values imply more homogeneous droplet distributions. In the our case the value was 0.89, which is indicative of the narrowness of the droplet size distribution (Arancibia et al., 2017), as also can be seen in Fig. 7. It was fairly constant for the 4 weeks, exhibiting a monomodal distribution with a small tail.

The Z-potential values changed from −32.80 at t = 0 to −40.17 mV after 30 days of storage. XG is anionic hydrocolloid at the neutral pH of the OOME, being DATEM a negative emulsifier covering the surface of droplets. The strong electrostatic repulsion forces existing between emulsifier and stabilizer helps to prevent droplet aggregation. Therefore, the optimal OOME can be considered stable in terms of colloidal

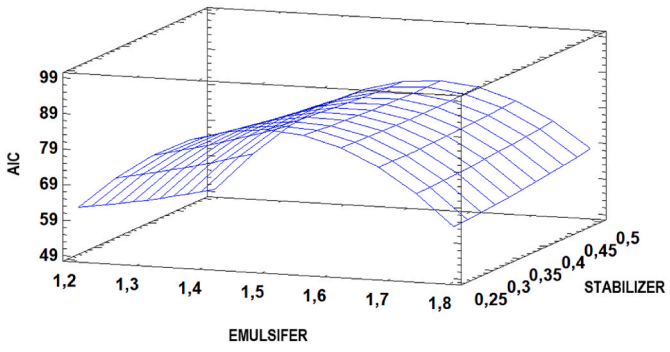

Fig. 6. Estimated response surface for emulsifier (%) and stabilizer (%) concentration optimization on AIC (mg/L) of the prepared emulsions for a buffer concentration of 400 mM.

Table 6
Desirability optimization of emulsifier (%), stabilizer (%) and buffer (mM) to minimize $d_{4/3}$ (μm) and maximize the AIC (mg/L) of the OOME.

Factor	Lowest	Highest	Optimal
Emulsifier (%)	1.25	1.75	1.466
Stabilizer (%)	0.25	0.5	0.250
Buffer (mM)	100.0	700.0	573.102

Table 7
Evolution of $d_{4/3}$ and AIC for 30 days since date of production of OOME.

Time (days)	0	7	14	22	30
$d_{4/3}$ (nm)	298 ± 4	317 ± 2	349 ± 4	314 ± 1	329 ± 1
AIC (mg/L)	108 ± 3	112 ± 6	104 ± 4	96 ± 4	98 ± 6

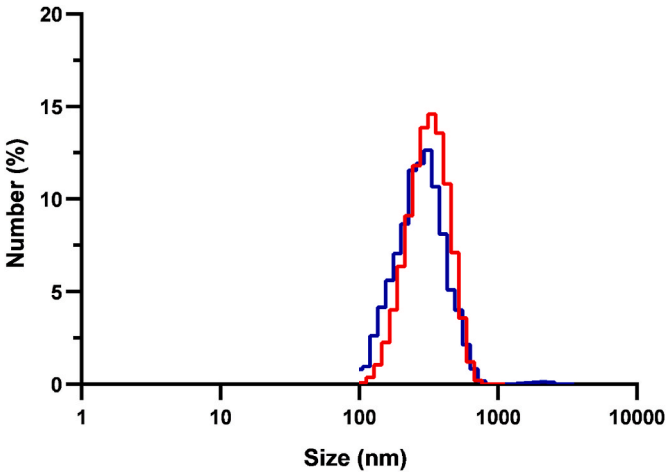

Fig. 7. Droplet size distribution of the OOME at day 0 (blue) and day 30 (red). (For interpretation of the references to color in this figure legend, the reader is referred to the Web version of this article.)

interactions against coalescence (Guzmán et al., 2021). However, these results do not guarantee OOME stability, since there are other factors that may affect physical stability. For this reason, stability of the optimal OOME for 30 days was also evaluated by the BS evolution over time using Turbiscan AGS apparatus to detect possible creaming, sedimentation, coalescence or flocculation. The Delta-BS (ΔBS) profiles monitored during 30 days at 25 °C are depicted in Fig. 8. Lines of different colors in the spectra represent the changes in the light transmittance of the optimal OOME at different times. In this figure, 3 regions can be clearly identified regarding emulsion instability phenomena: (1) on the left side there is a decrease in ΔBS, which is indicative of clarification (2) in the mid of the graph, a very slight variation in ΔBS, associated to discrete increase in particle size, and (3) a significant increase in ΔBS in the right part, which is a show of a creaming effect. However, the minor increase in ΔBS in the central part suggests a high stability of the OOME and that the little creaming effect is produced by particle migration. In turn, this is consistent with the maintenance of the $d_{4/3}$ with time measured by LLS depicted in Table 7.

The Turbiscan Stability Index (TSI) parameter is used for the evaluation of physical stability in dispersed systems. TSI considers all the phenomena that occur in the sample, obtaining an average value at each sampling point which allows to create a physical stability curve during the storage of the emulsion. The lower the TSI values, the more stable the emulsion. When 0.5≤TSI<2, the stability level is defined as good; when 2≤TSI<4, it is defined as general (Zhang et al., 2022). The TSI curve indicates that the OOME is physically stable, with TSI lower than 4 during 30 days storage, as shown in Fig. 9.

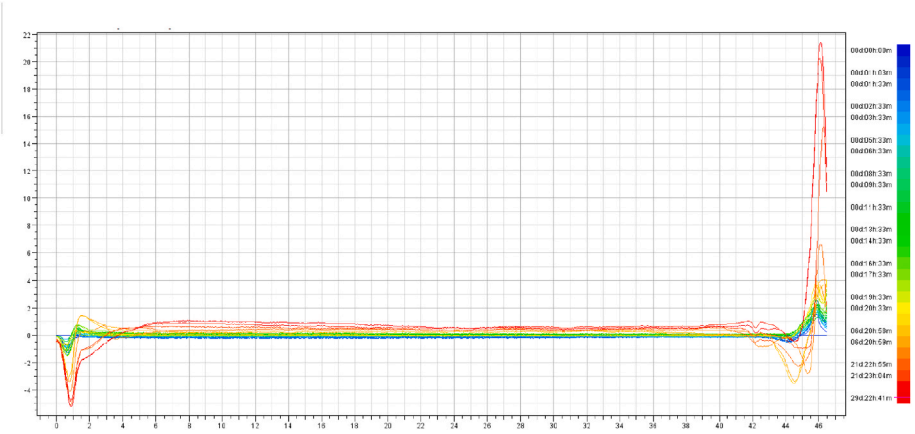

Fig. 8. Turbiscan Lab spectra showing Delta-BS (%) of the optimal OOME as a function of sample height (0–46 mm).

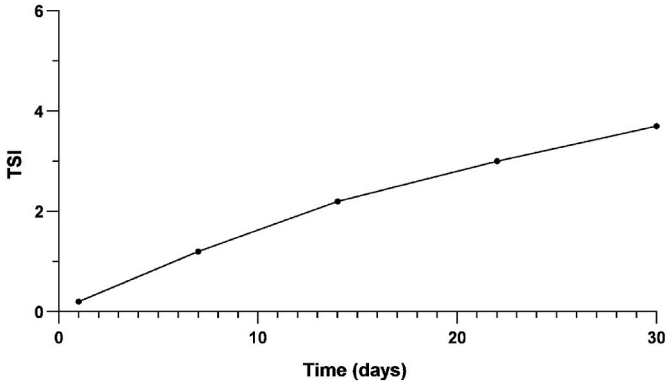

Fig. 9. TSI values of the optimal OOME within 30 days.

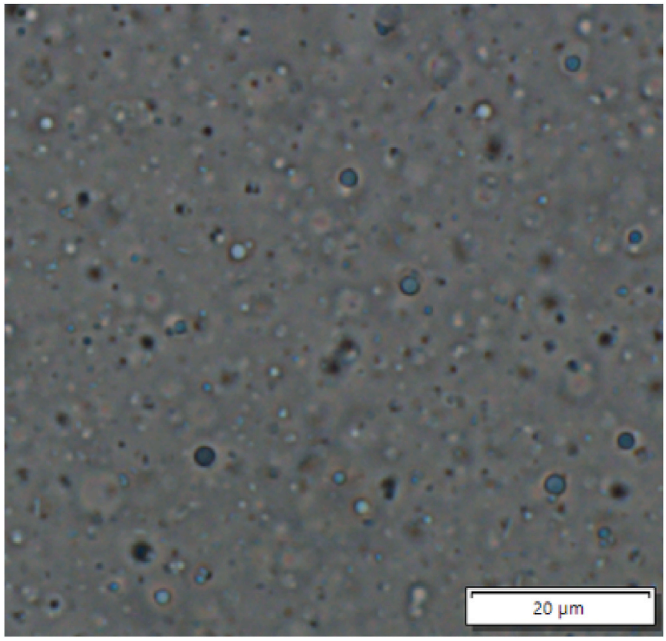

Fig. 10. Polarized light optical microscopy image of the OOME sample after 30 days of storage. Magnification 37.8×.

However, TSI values changed very significantly depending on the height. In the mid of the sample, TSI was below 1 up to 30 days of storage, which is indicative of an absence of flocculation or coalescence (Huang et al., 2021). On top of the sample, TSI after 30 days was also below 2, but slightly higher compared to the medium zone. In this zone, BS rose during storage, which means that the concentration of droplets increased at the top of the emulsion and, accordingly, a creaming phenomenon occurred. However, the intensity of BS at the bottom of OOME decreased with the time, suggesting that the clarification phenomenon appeared and that the slight instability of the emulsion was mainly caused by gravity separation (Niknam et al., 2020). In conclusion, the optimal OOME prepared did not show any considerable destabilization process during the storage period. Furthermore, even after 90 days, the sample was also macroscopically stable, maintaining the same milky color and homogeneous appearance, without creaming or phase separation.

Finally, the optimal OOME was observed under cross-polarized light microscopy. As can be seen in Fig. 10, the analysis of the sample did not detect birefringence but confirmed optical isotropy, typical of MEs (Barreto et al., 2022). The distribution and dimensions of droplets can also be assessed, confirming the emulsion is non-flocculated as the droplets are spherically shaped globules, homogenously distributed with a relatively small size.

3.3. Biological activities of OOME

Despite certain phytochemicals can suppress tumor cell growth or effect enzymes involved in carcinogen inactivation, they do not use to produce the complete desired action because of low bioavailability and permeability, which hinders them to reach the target site. To overcome these drawbacks, MEs can be used as drug-delivery carriers because of their capacity to improve the permeability of anti-tumour compounds (Janani et al., 2022). Unlike other tumor cells, colorectal cancer cells are exposed directly to dietary ingredients. Thus, there is a growing interest in investigating the association between phytochemicals and colorectal cancer (CRC) (Li et al., 2015) and recent epidemiological studies have confirmed that *Allium* vegetables may have beneficial effects in treating cancer (Zhao et al., 2021).

Table 8
Antitumor activity of OOME formulation, OO, PTS and PTSO in HT-29, T-84 and SW-837 cells.

Cell line	IC_{50} OOME (mg/L)	IC_{50} OO (mg/L)	PTS	PTSO
HT-29 (human colon adenocarcinoma)	1.7 ± 1,1	65 ± 1.4	2.6	9.2
T-84 (human colon carcinoma)	6.7 ± 2.9	5.4 ± 3.7	3	6.8
SW-837 (human rectum adenocarcinoma)	12.9 ± 3.0	22.2 ± 3.5	25.1	24.1

As shown in Table 8, in T84 cells our results did not show significant differences between the formulations. However, the OOME formulation showed higher antiproliferative activity in HT-29 and SW-837 compared to the results obtained with OO not emulsified and with the activities exerted by pure PTS and PTSO in the same lines (Guillamón et al., 2023). Cytotoxic activity of C-Neg was also analyzed. As cell viability was higher than 97 %, C-Neg was not consider to possess anti-cancer properties. These results provide evidence that the OOME significantly improved the antitumor effect of the OO in HT-29 and SW-837 cells. Other authors also found that ME exerted improved antitumor activities of phytochemicals in cancer cells compared to standard formulations (Panyajai et al., 2022). This might be attributed to its physical characteristics, which allow that these formulations can be effectively internalized into the tumour cells and accumulated in the cytoplasm, increasing the therapeutic effect. The small particle size of the OOME may enhance the uptake of OSCs by the cells, thereby increasing the bioavailability. In addition, the OOME is composed of anionic microparticles, which can be endocytosed by interacting with the positive site of the proteins on the cell membrane and be captured by the cell due to the repulsive interactions with the negatively charged cell surface (Sánchez-López et al., 2019; Zheng et al., 2022).

Inflammation is a key response of the body to some diseases, including cancer, that involves the activation of mediators like cytokines, whose uncontrolled production may damage tissues or promote loss of functions (Dantas et al., 2021). Previous studies have reported that the pro-inflammatory cytokine IL-8 is also considered tumorigenic due to its pro-metastatic properties, and it is commonly produced by different human carcinoma cell lines, including HT-29 (Brú et al., 2009; Wang et al., 2012). Regarding anti-inflammatory cytokines, it has been shown that IL-4 inhibited HT-29 cells growth through the activation of Stat1, a transcription factor involved in cell viability and immune response (Song et al., 2021). Therefore, the modulation of the production of both cytokines is an important factor in the inflammatory processes associated to CRC progression.

To evaluate the anti-inflammatory effect, increasing concentrations of OOME and OO were tested on HT-29 cells stimulated by LPS. The levels of pro-inflammatory cytokine IL-8 and anti-inflammatory IL-4 produced by these cells at the different conditions were calculated. In both cases, C Neg did not interfere with cytokine production. Therefore, the results obtained emphasize that the cytokine modulatory activity of OOME was attributable to the properties of PTS+PTSO. As shown in Fig. 11, all concentrations of both OO and OOME were able to decrease the concentration of IL-8 compared to control+LPS, in a dose-dependent manner. Despite treatment with OO also decreased levels of IL-8, compared to OOME there were significant differences in some doses ≤4 mg/L. In line with these findings, the anti-inflammatory capability of PTS and PTSO in colon cancer cell lines has previously been described by Vezza et al. (2019), who reported a reduction in IL-8 in Caco-2 cells. In addition, the separate abilities of PTS and PTSO have been documented in reducing other pro-inflammatory interleukins such as IL-6, observed in both cell lines and murine models (Liebana-García et al., 2022). This suggests a potential regulatory impact on the inflammatory cascade at both the cellular and *in vivo* levels.

Regarding IL-4, all concentrations tested of OO decreased the production of this cytokine in a dose dependent manner showing significant differences compared to C+LPS in all the concentrations tested (Fig. 12). However, OOME concentrations from 1 to 4 mg/L increased the production of this anti-inflammatory cytokine compared to C+LPS. These findings showed the immunomodulatory properties of these *Allium* compounds, which act differently depending on the concentration and the environmental circumstances (Schepetkin et al., 2019).

This increase in cytokines modulation by OOME in relation to ME can be attributed to the smaller droplet size and increased surface area. In this way, we were able to obtain a stable OOME with immunomodulatory and antitumor effects that could be applied in liquid nutraceutical compositions. However, new studies, including bioavailability or *in vivo* tests, should be carried out to better understand the performance of the developed OOME and confirm its potential pharmaceutical applications.

4. Conclusion

The present research defined the development and optimization of an OOME with antitumor and immunomodulatory effect. OOME was designed proposing a BBD modeling for optimization of amounts of emulsifier, stabilizer and buffer to minimize droplet size and maximize a maximum chemical stability. The stability of the optimal OOME was assessed by means of chemical and physical analysis over 30 days. The OOME improved the antiproliferative activity of OO in colorectal cell lines HT-29 and SW-837, as well as its influence on the inflammatory

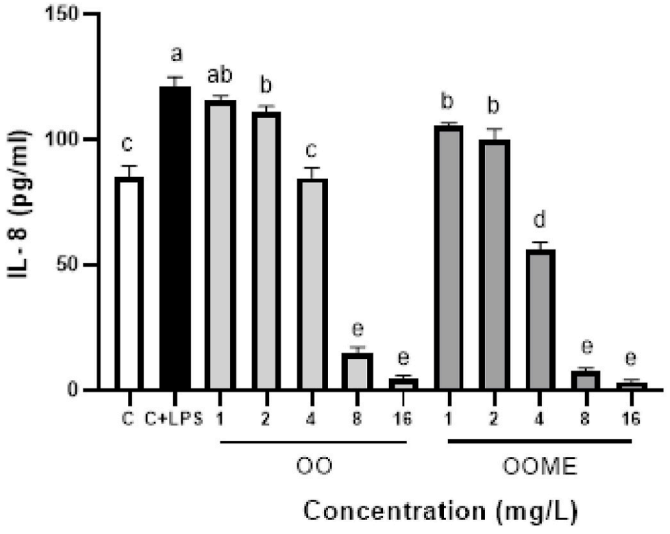

Fig. 11. Effect of OO and OOME on levels of IL-8 (pg/ml) produced by HT-29 cells. Cells were induced with LPS (10 μg/ml) and increasing concentrations of OO and OOME (1–16 mg/L of PTS+PTSO) for 24h. C: cells not induced with LPS (Control), C+LPS: cells induced with LPS. Groups with different letters are significantly different ($p < 0.05$).

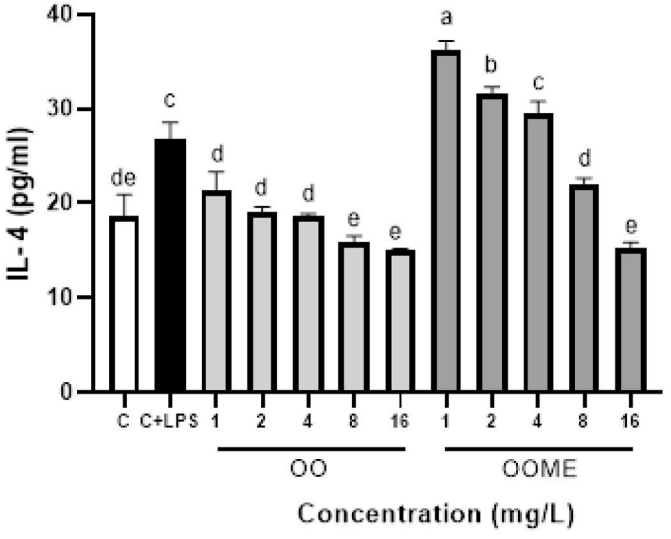

Fig. 12. Effect of OO and OOME on levels of IL-4 (pg/ml) produced by HT-29 cells. Cells were induced with LPS (10 μg/ml) and increasing concentrations of OO and OOME (1–16 mg/L of PTS+PTSO) for 24h. C: cells not induced with LPS (Control), C+LPS: cells induced with LPS. Groups with different letters are significantly different ($p < 0.05$).

response, with a reduction in the levels of pro-inflammatory cytokine IL-8 at all concentrations of OOME tested compared to OO or to control+LPS. In summary, the prepared OOME could improve the solubility, stability, antitumor activity and immune-boosting effect of its OSCs (PTS+PTSO). This OOME might be a promising liquid delivery system to be applied in nutraceutical compositions to provide immunomodulatory or antitumor effects, though further *in vivo* and bioavailability tests should be carried out to confirm its potential pharmaceutical applications.

Funding

This work was supported by the MISIONES-CDTI program (CDTI, Centre for the Development of Industrial Technology; Grant number MIG-20201012).

CRediT authorship contribution statement

Enrique Guillamon Ayala: Conceptualization, Investigation, Methodology, Writing – original draft. **Borja Domínguez Martín:** Investigation. **Nuria Mut-Salud:** Investigation, Methodology, Writing – review & editing. **Javier M. Ochando-Pulido:** Writing – review & editing. **José Antonio Morales-González:** Data curation. **Alberto Baños Arjona:** Conceptualization, Formal analysis, Funding acquisition. **Antonio Martinez-Ferez:** Conceptualization, Formal analysis, Writing – review & editing.

Declaration of competing interest

The authors declare that they have no known competing financial interests or personal relationships that could have appeared to influence the work reported in this paper.

Data availability

No data was used for the research described in the article.

Acknowledgment

The authors would like to thank to Dr. María Arántzazu Aguinaga for her comments and suggestions during manuscript's writing.

References

Abad, P., Arroyo-Manzanares, N., & García-Campaña, A. M. (2016). A rapid and simple UHPLC-ESI-MS/MS method for the screening of propyl propane thiosulfonate, a new additive for animal feed. *Analytical Methods, 8*(18), 3730–3739. https://doi.org/10.1039/C6AY00219F

Arancibia, C., Miranda, M., Matiacevich, S., & Troncoso, E. (2017). Physical properties and lipid bioavailability of nanoemulsion-based matrices with different thickening agents. *Food Hydrocolloids, 73*, 243–254. https://doi.org/10.1016/j.foodhyd.2017.07.010

Arredondo-Ochoa, T., & Silva-Martínez, G. A. (2022). Microemulsion based nanostructures for drug delivery. *Frontiers in Nanotechnology, 3*. https://www.frontiersin.org/articles/10.3389/fnano.2021.753947.

Arshad, M. S., Sohaib, M., Nadeem, M., Saeed, F., Imran, A., Javed, A., Amjad, Z., & Batool, S. M. (2017). Status and trends of nutraceuticals from onion and onion by-products: A critical review. *Cogent Food & Agriculture, 3*(1), Article 1280254. https://doi.org/10.1080/23311932.2017.1280254

Barreto, I. C., Costa, S. P. M., de Jesus Santos, A., Farias, A. P., Sarmento, V. H. V., Teodoro, A. V., de Souza Nunes, R., & Guedes de Sena Filho, J. (2022). Incorporation of essential oil from Vitex gardneriana (Lamiaceae) in microemulsions systems based on mineral and cottonseed oils increased its bioactivity against a coconut pest mite. *Industrial Crops and Products, 183*, Article 114963. https://doi.org/10.1016/j.indcrop.2022.114963

Brú, A., Souto, J.-C., Alcolea, S., Antón, R., Remacha, A., Camacho, M., Soler, M., Brú, I., Porres, A., & Vila, L. (2009). Tumour cell lines HT-29 and FaDu produce proinflammatory cytokines and activate neutrophils in vitro: Possible applications for neutrophil-based antitumour treatment. *Mediators of Inflammation.* , Article 817498. https://doi.org/10.1155/2009/817498, 2009.

Cai, Y., Deng, X., Liu, T., Zhao, M., Zhao, Q., & Chen, S. (2018). Effect of xanthan gum on walnut protein/xanthan gum mixtures, interfacial adsorption, and emulsion properties. *Food Hydrocolloids, 79*, 391–398. https://doi.org/10.1016/j.foodhyd.2018.01.006

Carbone, C., Musumeci, T., Lauro, M. R., & Puglisi, G. (2015). Eco-friendly aqueous core surface-modified nanocapsules. *Colloids and Surfaces B: Biointerfaces, 125*, 190–196. https://doi.org/10.1016/j.colsurfb.2014.11.038

Dai, L., Hinrichs, J., & Weiss, J. (2020). Ionic strength and pH stability of oil-in-water emulsions prepared with acid-hydrolyzed insoluble proteins from *Chlorella protothecoides*. *Journal of the Science of Food and Agriculture, 100*(4237), 4244. https://doi.org/10.1002/jsfa.10464

Dantas, A. G. B., de Souza, R. L., de Almeida, A. R., Xavier Júnior, F. H., Pitta, M. G. da R., Rêgo, M. J. B. de M., & Oliveira, E. E. (2021). Development, characterization, and immunomodulatory evaluation of carvacrol-loaded nanoemulsion. *Molecules, 26*(13), 3899. https://doi.org/10.3390/molecules26133899

Girish Sharma, G. S., Dhan Prakash, D. P., & Charu Gupta, C. G. (2014). Phytochemicals of nutraceutical importance: Do they defend against diseases? *Phytochemicals of Nutraceutical Importance*, 1–19. https://doi.org/10.1079/9781780643632.0001

Guillamon, E. (2018). Efecto de compuestos fitoquímicos del género Allium sobre el sistema inmune y la respuesta inflamatoria. *Ars Pharmaceutica, 59*(3), 3.

Guillamón, E., Mut-Salud, N., Rodríguez-Sojo, M. J., Ruiz-Malagón, A. J., Cuberos-Escobar, A., Martínez-Férez, A., Rodríguez-Nogales, A., Gálvez, J., & Baños, A. (2023). In vitro antitumor and anti-inflammatory activities of allium-derived compounds propyl propane thiosulfonate (PTSO) and propyl propane thiosulfinate (PTS). *Nutrients, 15*(6), 6. https://doi.org/10.3390/nu15061363

Gupta, C., & Prakash, D. (2015). Nutraceuticals for geriatrics. *Journal of Traditional and Complementary Medicine, 5*(1), 5–14. https://doi.org/10.1016/j.jtcme.2014.10.004

Guzmán, C., Rojas, M. A., & Aragón, M. (2021). Optimization of ultrasound-assisted emulsification of emollient nanoemulsions of seed oil of Passiflora edulis var. Edulis. *Cosmetics, 8*(1), 1. https://doi.org/10.3390/cosmetics8010001

Huang, K., Liu, R., Zhang, Y., & Guan, X. (2021). Characteristics of two cedarwood essential oil emulsions and their antioxidant and antibacterial activities. *Food Chemistry, 346*, Article 128970. https://doi.org/10.1016/j.foodchem.2020.128970

Janani, S. K., Sureshkumar, R., Dhanabal, S. P., Janani, S. K., Sureshkumar, R., & Dhanabal, S. P. (2022). Perspective chapter: Microemulsion as a game changer to conquer cancer with an emphasis on herbal compounds. In *Surfactants and detergents—updates and new insights*. IntechOpen. https://doi.org/10.5772/intechopen.101479.

Kianian, F., Marefati, N., Boskabady, M., Ghasemi, S. Z., & Boskabady, M. H. (2021). Pharmacological properties of Allium cepa, preclinical and clinical evidences; A review. *Iranian Journal of Pharmaceutical Research: International Journal of Psychological Research, 20*(2), 107–134. https://doi.org/10.22037/ijpr.2020.112781.13946

Kori, A. H., Mahesar, S. A., Sherazi, S. T. H., Khatri, U. A., Laghari, Z. H., & Panhwar, T. (2021). Effect of process parameters on emulsion stability and droplet size of pomegranate oil-in-water. *Grasas y Aceites, 72*(2), e410. https://doi.org/10.3989/gya.0219201

Kumar, A., Kaur, R., Kumar, V., Kumar, S., Gehlot, R., & Aggarwal, P. (2022). New insights into water-in-oil-in-water (W/O/W) double emulsions: Properties, fabrication, instability mechanism, and food applications. *Trends in Food Science & Technology, 128*, 22–37. https://doi.org/10.1016/j.tifs.2022.07.016

Li, Y.-H., Niu, Y.-B., Sun, Y., Zhang, F., Liu, C.-X., Fan, L., & Mei, Q.-B. (2015). Role of phytochemicals in colorectal cancer prevention. *World Journal of Gastroenterology, 21*(31), 9262–9272. https://doi.org/10.3748/wjg.v21.i31.9262

Liébana-García, R., Olivares, M., Rodríguez-Ruano, S. M., Tolosa-Enguís, V., Chulia, I., Gil-Martínez, L., Guillamón, E., Baños, A., & Sanz, Y. (2022). The Allium derivate propyl propane thiosulfinate exerts anti-obesogenic effects in a murine model of diet-induced obesity. *Nutrients, 14*(3), 440. https://doi.org/10.3390/nu14030440

Long, Z., Zhao, Q., Liu, T., Kuang, W., Xu, J., & Zhao, M. (2013). Influence of xanthan gum on physical characteristics of sodium caseinate solutions and emulsions. *Food Hydrocolloids, 32*(1), 123–129. https://doi.org/10.1016/j.foodhyd.2012.12.017

Lu, Y., Kang, W., Jiang, J., Chen, J., Xu, D., Zhang, P., Zhang, L., Feng, H., & Wu, H. (2017). Study on the stabilization mechanism of crude oil emulsion with an amphiphilic polymer using the β-cyclodextrin inclusion method. *RSC Advances, 7*(14), 8156–8166. https://doi.org/10.1039/C6RA28528G

McClements, D. J., & Jafari, S. M. (2018). Improving emulsion formation, stability and performance using mixed emulsifiers: A review. *Advances in Colloid and Interface Science, 251*, 55–79. https://doi.org/10.1016/j.cis.2017.12.001

Nagy, P., & Winterbourn, C. C. (2010). Chapter 6—redox chemistry of biological thiols. In J. C. Fishbein (Ed.), *Advances in molecular toxicology, 4* pp. 183–222). Elsevier. https://doi.org/10.1016/S1872-0854(10)04006-3.

Niknam, S. M., Escudero, I., & Benito, J. M. (2020). Formulation and preparation of water-in-oil-in-water emulsions loaded with a phenolic-rich inner aqueous phase by application of high energy emulsification methods. *Foods, 9*(10), 1411. https://doi.org/10.3390/foods9101411

Panyajai, P., Chueahongthong, F., Viriyaadhammaa, N., Nirachonkul, W., Tima, S., Chiampanichayakul, S., Anuchapreeda, S., & Okonogi, S. (2022). Anticancer activity of Zingiber ottensii essential oil and its nanoformulations. *PLoS One, 17*(1), Article e0262335. https://doi.org/10.1371/journal.pone.0262335

Raikos, V., Duthie, G., & Ranawana, V. (2017). Comparing the efficiency of different food-grade emulsifiers to form and stabilise orange oil-in-water beverage emulsions: Influence of emulsifier concentration and storage time. *International Journal of Food Science and Technology, 52*(2), 348–358. https://doi.org/10.1111/ijfs.13286

Sánchez-López, E., Guerra, M., Dias-Ferreira, J., Lopez-Machado, A., Ettcheto, M., Cano, A., Espina, M., Camins, A., Garcia, M. L., & Souto, E. B. (2019). Current applications of nanoemulsions in cancer therapeutics. *Nanomaterials, 9*(6), 821. https://doi.org/10.3390/nano9060821

Santos, J., Trujillo-Cayado, L. A., Carrillo, F., López-Castejón, M. L., & Alfaro-Rodríguez, M. C. (2022). Relation between droplet size distributions and physical stability for zein microfluidized emulsions. *Polymers, 14*(11), 2195. https://doi.org/10.3390/polym14112195

Schepetkin, I. A., Kirpotina, L. N., Khlebnikov, A. I., Balasubramanian, N., & Quinn, M. T. (2019). Neutrophil immunomodulatory activity of natural organosulfur compounds. *Molecules, 24*(9), 1809. https://doi.org/10.3390/molecules24091809

Song, X., Traub, B., Shi, J., & Kornmann, M. (2021). Possible roles of interleukin-4 and -13 and their receptors in gastric and colon cancer. *International Journal of Molecular Sciences, 22*(2), 727. https://doi.org/10.3390/ijms22020727

Sorlozano-Puerto, A., Albertuz-Crespo, M., Lopez-Machado, I., Gil-Martinez, L., Ariza-Romero, J. J., Maroto-Tello, A., Baños-Arjona, A., & Gutierrez-Fernandez, J. (2020). Antibacterial and antifungal activity of propyl-propane-thiosulfinate and propyl-propane-thiosulfonate, two organosulfur compounds from Allium cepa: In vitro antimicrobial effect via the gas phase. *Pharmaceuticals, 14*(1), 1. https://doi.org/10.3390/ph14010021

Souto, E. B., Cano, A., Martins-Gomes, C., Coutinho, T. E., Zielińska, A., & Silva, A. M. (2022). Microemulsions and nanoemulsions in skin drug delivery. *Bioengineering, 9*(4), 158. https://doi.org/10.3390/bioengineering9040158

Taghavi, E., Abdul Salam, A. S., Anarjan, N., Nillian, E., & Lani, M. N. (2022). Onion essential oil-in-water emulsion as a food flavoring agent: Effect of environmental stress on physical properties and antibacterial activity. *International Journal of Food Science, 2022*, Article e1363590. https://doi.org/10.1155/2022/1363590

Vega, E. D., Vásquez, E., Díaz, J. R. A., & Masuelli, M. A. (2015). Influence of the ionic strength in the intrinsic viscosity of xanthan gum. An experimental review. *Journal of Polymer and Biopolymer Physics Chemistry, 3*(1), 12–18.

Vezza, T., Algieri, F., Garrido-Mesa, J., Utrilla, M. P., Rodríguez-Cabezas, M. E., Baños, A., Guillamón, E., García, F., Rodríguez-Nogales, A., & Gálvez, J. (2019). The immunomodulatory properties of propyl-propane thiosulfonate contribute to its intestinal anti-inflammatory effect in experimental colitis. *Molecular Nutrition & Food Research, 63*(5), 5. https://doi.org/10.1002/mnfr.201800653

Vezza, T., Garrido-Mesa, J., Diez-Echave, P., Hidalgo-García, L., Ruiz-Malagón, A. J., García, F., Sánchez, M., Toral, M., Romero, M., Duarte, J., Guillamón, E., Baños Arjona, A., Moron, R., Galvez, J., Rodríguez-Nogales, A., & Rodríguez-Cabezas, M. E. (2021). Allium-derived compound propyl propane thiosulfonate (PTSO) attenuates metabolic alterations in mice fed a high-fat diet through its anti-inflammatory and prebiotic properties. *Nutrients, 13*(8), 2595. https://doi.org/10.3390/nu13082595

Vichai, V., & Kirtikara, K. (2006). Sulforhodamine B colorimetric assay for cytotoxicity screening. *Nature Protocols, 1*(3), 3. https://doi.org/10.1038/nprot.2006.179

Wang, H., Khor, T. O., Shu, L., Su, Z.-Y., Fuentes, F., Lee, J.-H., & Kong, A.-N. T. (2012). Plants vs. cancer: A review on natural phytochemicals in preventing and treating cancers and their druggability. *Anti-Cancer Agents in Medicinal Chemistry, 12*(10), 1281–1305. https://doi.org/10.2174/187152012803833026

Yang, H., Kang, W., Yu, Y., Yin, X., Wang, P., & Zhang, X. (2017). A new approach to evaluate the particle growth and sedimentation of dispersed polymer microsphere profile control system based on multiple light scattering. *Powder Technology, 315*, 477–485. https://doi.org/10.1016/j.powtec.2017.04.001

Yerramilli, M., & Ghosh, S. (2017). Long-term stability of sodium caseinate-stabilized nanoemulsions. *Food Science & Technology (New York), 54*, 82–92. https://doi.org/10.1007/s13197-016-2438-y

Zhang, M., Fan, L., Liu, Y., & Li, J. (2022). A mechanistic investigation of the effect of dispersion phase protein type on the physicochemical stability of water-in-oil emulsions. *Food Research International, 157*, Article 111293. https://doi.org/10.1016/j.foodres.2022.111293

Zhao, X.-X., Lin, F.-J., Li, H., Li, H.-B., Wu, D.-T., Geng, F., Ma, W., Wang, Y., Miao, B.-H., & Gan, R.-Y. (2021). Recent advances in bioactive compounds, health functions, and safety concerns of onion (Allium cepa L.). *Frontiers in Nutrition, 8*, Article 669805. https://doi.org/10.3389/fnut.2021.669805

Zheng, L., Cao, C., Li, R.-Y., Cao, L.-D., Zhou, Z.-L., Li, M., & Huang, Q.-L. (2018). Preparation and characterization of water-in-oil emulsions of isoprothiolane. *Colloids and Surfaces A: Physicochemical and Engineering Aspects, 537*, 399–410. https://doi.org/10.1016/j.colsurfa.2017.10.031

Zheng, Y., Xu, G., Ni, Q., Wang, Y., Gao, Q., & Zhang, Y. (2022). Microemulsion delivery system improves cellular uptake of genipin and its protective effect against aβ1-42-induced PC12 cell cytotoxicity. *Pharmaceutics, 14*, 617. https://doi.org/10.3390/pharmaceutics14030617